

Semi-Analytical Modeling for Interior Permanent Magnet Synchronous Machines Considering Permeability of Rotor Core

Shin, Kyung-Hun; Wang, Bingnan

TR2020-149 November 25, 2020

Abstract

This paper propose an improved semi-analytical model based on subdomain method for the performance analysis of an interior permanent magnet synchronous machine. In particular, the pole-piece and the bridge region of the rotor were modeled with finite permeability. This enables the calculation of magnetic field in the core region to account for the saturation effect, and improves the accuracy of the motor electromagnetic performance calculation

International Conference on Electrical Machines and Systems (ICEMS) 2020

Semi-Analytical Modeling for Interior Permanent Magnet Synchronous Machines Considering Permeability of Rotor Core

Kyung-Hun Shin^{1,2}, and Bingnan Wang¹

¹ Mitsubishi Electric Research Laboratories, 201 Broadway, Cambridge, MA 02139, USA

² Department of Electrical and Computer Engineering, University of Illinois at Urbana-Champaign, Urbana, IL 61801, USA

Abstract—This paper propose an improved semi-analytical model based on subdomain method for the performance analysis of an interior permanent magnet synchronous machine. In particular, the pole-piece and the bridge region of the rotor were modeled with finite permeability. This enables the calculation of magnetic field in the core region to account for the saturation effect, and improves the accuracy of the motor electromagnetic performance calculation.

Index Terms—Interior permanent magnet synchronous machine, magnetic modeling, subdomain method.

I. INTRODUCTION

Interior permanent magnet synchronous machines (IPMSMs) are becoming a popular choice in various applications, such as robotics, drive train, wind turbine, elevator, and home appliances [1], due to many advantages that IPMSM can offer. Because of the rotor's magnetic saliency, interior permanent magnet synchronous machines (IPMSMs) not only have a high torque density per permanent magnet usage, but also have a wide operating range [2], [3], [4]. It is therefore essential to develop appropriate analysis and design methods for the development of new IPMSMs.

Finite-element (FE) based simulations are widely used by motor designers, which can achieve very high accuracy, but are computationally intensive and time-consuming, and therefore not suitable for optimizing the many design parameters of a motor in the initial design stage. On the other hand, analytical based approaches offer rapid analysis with various reduced order modeling techniques, and can be useful in initial design evaluation and optimization. Analytical based methods that have been investigated for the magnetic modeling include magnetic equivalent circuit (MEC), relative permeance models, complex permeance models, and subdomain method [5], [6]. MEC technique can be implemented quickly and simply for design optimization. However, its accuracy suffers because of oversimplification. The latter three methods all solve for the partial differential equation (PDE) of a magnetic potential that is derived from Maxwell's equations. Separation of variables and Fourier series are often used to find closed form solutions for these governing PDEs. Compared with the relative permeance model and complex permeance model, which adopts the same

permeance function for any rotor position to account for the slotting effect, the subdomain models evaluate the influence of slotting for each rotor position, which makes it is more accurate [7].

A lot of work have been developed toward the analytical based modeling method for surface-mounted PM (SMPM) machines and switched reluctance machines [8], [9], [10]. However, when compared to surface-mounted PM machines, the complex IPM rotor structures increase the difficulty of the design. It is also challenging to describe IPM machines using an effective analytical model because the flux path in the rotor structure is difficult to predict. Actually most of the analytical models available deal with the magnetic field in the air gap region only, and treat the permeability of the iron core as infinity. In previous studies a simplified subdomain model have been developed for an IPMSM machine; however, the core region was still not included in the calculation domains [11]. Very recently the finite permeability of ferromagnetic materials was considered in an iron-cored coil [12], and a spoke-type motor [13]. However, the modeling of iron core of IPMSM has not been reported so far to the best of our knowledge.

This paper proposes an improved subdomain method with finite permeability of rotor of an IPMSM, which enables the calculation of magnetic field in the core region, and more accurate evaluation of the electromagnetic performances such as back electromotive force (EMF) and instantaneous torque. Using nonlinear FE simulation as a benchmark, the accuracy of proposed analysis method is validated.

II. THE PROPOSED MODEL

The subdomain method solves for the governing equation of magnetic vector potential (MVP) in the framework of magneto-static approximation of Maxwell's equations. First the actual structure of the IPMSM is simplified for easier treatment in 2D polar coordinates. Then the structure is divided into subdomains, with the source terms described by magnetization and surface current density respectively, and the governing equations and the general solutions provided by Fourier series. Then the boundary conditions between subdomains are used to identify the unknown coefficients. The

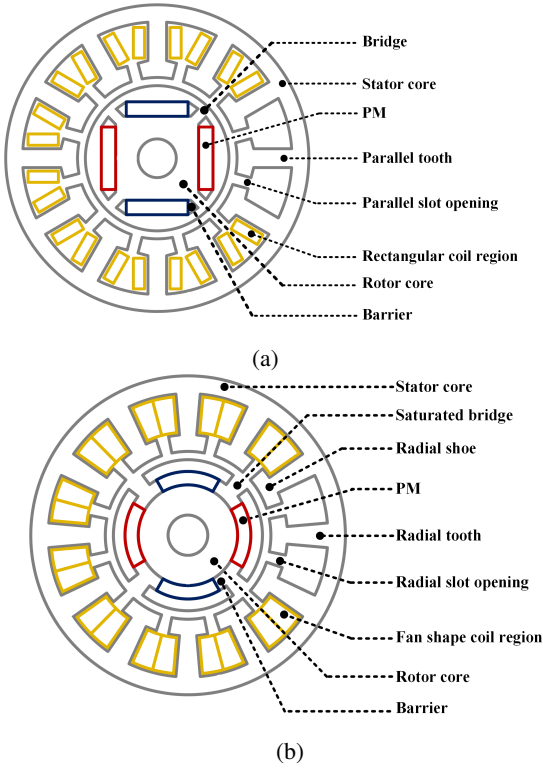


Fig. 1: (a) The original IPMSM topology, and (b) the simplified IPMSM topology for analytical modeling purpose.

electromagnetic performances can be derived subsequently once the MVP is obtained.

Fig. 1(a) shows the actual structure of IPMSM, and a simplified model for the purpose of the analysis is shown in Fig. 1(b). The following basic assumptions are adopted in the formulation of the analytical model: end effects along the z -axis direction are neglected, and the structures all have radial sides, including the stator slots and openings, and the PMs in the rotor. Under the magneto-static approximation, eddy-current effect is not considered, and the conductivity of materials is neglected. For the magnetic properties of materials, we assume that the PMs have the same relative permeability as air, which is equal to one; the relative permeability of the steel cores of the stator and rotor are infinite.

In IPMSM machine, the accurate modeling of bridge region due to saturation is critical in predicting the performance of a design. Previous analytical model assumed that the permeability of the bridge region was the same as that of vacuum, while the pole pieces are assumed to be infinitely permeable. For this reason, the error of the analysis result was inevitable. In this work, we divide the pole-piece and bridge regions into separate subdomains, and finite permeability values are assigned to each subdomain. For the saturated bridge region, the relative permeability is determined by the B-H curve of the core material. With this setting, iterative method can be used to account for the nonlinear effect and

identify the permeability of the saturated region at different operating conditions.

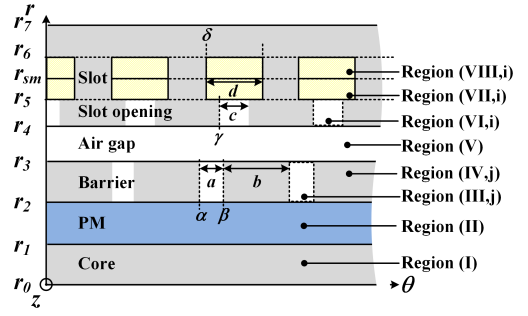


Fig. 2: The subdomain regions for the the analysis of IPMSM motor.

As shown in Fig. 2, based on the simplified structure, we divide the whole geometry into different subdomains: Region I (the rotor core subdomain), Region II (the PM subdomain), Regions III, j ($j = 1, 2, \dots, 2p$) (the j -th barrier subdomains), Regions IV, j (the j -th pole-piece subdomains), Regions VI, i ($i = 1, 2, \dots, Q$) (the i -th slot-opening subdomains), Regions VII, i (the i -th bottom slot subdomains), Regions VIII, i (the i -th top slot subdomains), and Regions V (the air-gap subdomains). Regions I, II, and V have periodic shapes and are homogeneous in the tangential direction.

A single partial differential equation (PDE) for magnetic vector potential can be derived from Maxwell's equations, where the magnetic vector potential \mathbf{A} is defined as

$$\nabla \times \mathbf{A} = \mathbf{B}, \quad (1)$$

where \mathbf{B} is the magnetic flux density. The PDE, referred to as the governing equation, in the regions of rotor core (I), barrier (III, j), pole-piece (VI, j), slot-opening (VI, i) and air gap (V) are represented as Laplace's equation; whereas the governing equations of the PM (II) and slot (VII, VIII) region are represented by Poisson's equation:

$$\begin{aligned} \nabla_z^2 \mathbf{A}_z^{\text{I}} &= 0 & \nabla_z^2 \mathbf{A}_z^{\text{II}} &= -\mu_0 (\nabla \times \mathbf{M}^{\text{II}}) \\ \nabla_z^2 \mathbf{A}_z^{\text{III},j} &= 0 & \nabla_z^2 \mathbf{A}_z^{\text{IV},j} &= 0 \\ \nabla_z^2 \mathbf{A}_z^{\text{V}} &= 0 & \nabla_z^2 \mathbf{A}_z^{\text{VI},i} &= 0 \\ \nabla_z^2 \mathbf{A}_z^{\text{VII},i} &= -\mu_0 \mathbf{J}^{\text{VII},i} & \nabla_z^2 \mathbf{A}_z^{\text{VIII},i} &= -\mu_0 \mathbf{J}^{\text{VIII},i} \end{aligned} \quad (2)$$

Note that the subdomains in this analytical model for IPMSM can be categorized into two types: periodic subdomains, including the air gap, shaft, and stator yoke, and non-periodic subdomains, including the stator slots and openings, the buried PMs, and the pole-piece and bridge regions. All these boundary conditions need to be matched in order to fully identify the specific solutions for each subdomain. The general solution of Laplace's equations in each subdomain is written in the form of Fourier series based on superposition principle, and needs to be written in a form according to the imposed boundary conditions [13].

To be more specific, we write the general solution for Laplace's equation in a subdomain with periodic boundary conditions as:

$$\mathbf{A}_z^h = (A_0 + B_0 \ln(r)) + \sum_{n=1} \left[\begin{aligned} & \left(A_n(r)^{-n} + B_n(r)^n \right) \cos(n\theta) \\ & + \left(C_n(r)^{-n} + D_n(r)^n \right) \sin(n\theta) \end{aligned} \right] \mathbf{i}_z, \quad (3)$$

where n is a harmonic number, and $A_0, B_0, A_n, B_n, C_n, D_n$, are the unknown coefficients to be determined.

On the other hand, for a subdomain with non-periodic boundaries, we write the general solution for Laplace's equation as:

$$\mathbf{A}_z^h = (A_0 + B_0 \ln(r)) + \sum_{k=1}^{\infty} \left(A_k(r)^{-k_k} + B_k(r)^{k_k} \right) \cos(k_k(\theta - \theta_1)) + \sum_{m=1} \left(\begin{aligned} & A_m \frac{\sinh(k_m(\theta - \theta_1))}{\sinh(k_m\zeta)} \\ & + B_m \frac{\sinh(k_m(\theta - \theta_2))}{\sinh(k_m\zeta)} \end{aligned} \right) \sin \left[k_m \ln \left(\frac{r}{r_i} \right) \right] \mathbf{i}_z \quad (4)$$

where k and m are the harmonic number, $k_k = k\pi/\zeta$, $k_m = m\pi/\ln(r_o/r_i)$, and r_i and r_o are the inner and outer radii of the subdomain respectively, ζ is angular width of the subdomain, θ_1 and θ_2 are the beginning and ending angular positions of the subdomain, respectively.

For subdomains with sources, the governing equation is in the form of Poisson's equation, as shown in Eq. 2. In this case, the solution of magnetic vector potential can be written as the summations of particular solutions due to the source, and the general solutions of the corresponding Laplace's equation without the source term.

The magnetic flux density components in the radial direction B_r and tangential direction B_θ can be obtained from magnetic vector potential, according to the definition Eq. 1, as

$$\mathbf{B}_r = \frac{1}{r} \frac{\partial A_z}{\partial \theta} \mathbf{i}_r, \quad \mathbf{B}_\theta = -\frac{\partial A_z}{\partial r} \mathbf{i}_\theta \quad (5)$$

After obtaining the general solutions for all the subdomains, the unknown coefficients in the solutions will need to be identified using boundary conditions. In general, from Maxwell's equations, the behavior of the magnetic field at the boundary between domains χ and $\chi + 1$ can be expressed as

$$\mathbf{n} \cdot (\mathbf{B}^{(\chi)} - \mathbf{B}^{(\chi+1)}) = 0 \quad (6)$$

$$\mathbf{n} \times (\mathbf{H}^{(\chi)} - \mathbf{H}^{(\chi+1)}) = \mathbf{J}_s \quad (7)$$

where \mathbf{J}_s is the current density on the boundary surface, and \mathbf{n} is the unity vector normal to that boundary. The continuity of the normal component of the magnetic flux density (Eq. 6) can be mathematically simplified as the continuity of the magnetic vector potential (\mathbf{A}_z) at both interfaces is the same [5].

The boundaries that need to be matched for the IPMSM model are illustrated in Fig. 3. The detailed equations for all

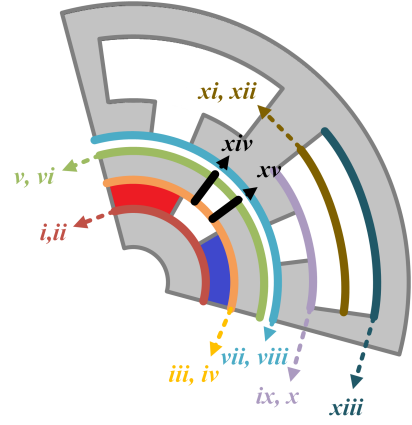


Fig. 3: The boundary conditions that need to be considered for the calculation of the solutions.

the boundaries are not listed here. Special attention need to be paid for the boundaries between the pole-pieces and bridge regions, where both boundaries in the radial and tangential directions need to be matched. In particular, the boundaries in the radial direction that need to be matched are written as:

$$xiv) \theta = \alpha_j + a = \beta_j : \quad A_z^{III,j}(r, \alpha_j + a) = A_z^{IV,j}(r, \beta_j) \quad (8)$$

$$H_r^{III,j}(r, \alpha_j + a) = H_r^{IV,j}(r, \beta_j) \quad (9)$$

$$xv) \theta = \alpha_{j+1} = \beta_j + b : \quad A_z^{III,j+1}(r, \alpha_{j+1}) = A_z^{IV,j}(r, \beta_j + b) \quad (10)$$

$$H_r^{III,j+1}(r, \alpha_{j+1}) = H_r^{IV,j}(r, \beta_j + b) \quad (11)$$

The unknown coefficients can then be determined by solving the system of linear equations obtained from the boundary conditions between various subdomains. After that, the solution for the magnetic vector potential in the whole calculation domain is fully determined. All the electromagnetic performance metrics of the IPMSM, including the magnetic flux density distribution, the flux linkage, the back electromotive force (EMF), the cogging torque, and the generated electromagnetic torque, can be derived directly from the magnetic vector potential solution [5].

III. RESULTS & DISCUSSION

The calculation model proposed in the previous session is implemented. The detailed parameters of the analysis model for the IPMSM are listed in Table I. In order to achieve good precision in the analytical evaluation, the number of harmonic orders used in the computations are $N = 100$ (account for the air-gap and PM subdomains) and $V = M = K = 5$ (account for the barrier, pole-piece, slots, and slot-opening subdomains).

The calculation results from the proposed analytical model are plotted together with the nonlinear FE simulation. Fig. 4 compares the back-EMF at no-load condition, while Fig. 5 plots the electromagnetic torque generated by the motor with three phase armature current waveform, over the time of

TABLE I: List of parameters of the IPMSM model.

Parameter	Value	Parameter	Value
r_0	10 mm	a	9°
r_1	20 mm	B	51°
r_2	23 mm	c	3.37°
r_3	25 mm	d	5.3°
r_4	25.5 mm	μ_r^{III}	2
r_5	26.5 mm	μ_r^{IV}	1000
r_6	40.5 mm	ω_r	1000 rpm
r_4	50 mm	I_p	25 A

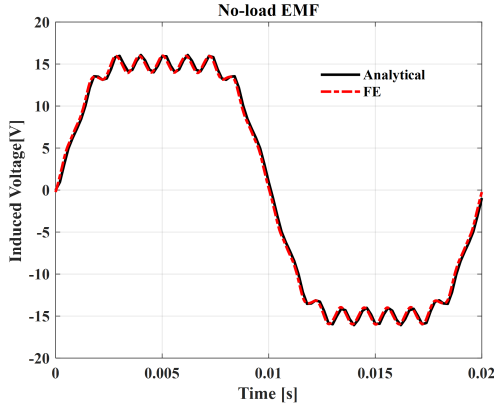


Fig. 4: The calculated back-EMF at no load condition over one electrical cycle, for both analytical and FE calculations.

one electrical cycle. From the figures we can see the results from the proposed model are in good agreement with the FE simulation results at all rotor positions, and the relative error is within 1%.

It is worth to note that, for a given rotor position, the computation time is approximately 1 second with the analytical model, whereas the nonlinear FE analysis takes approximately 30 seconds with 45,700 elements. Therefore, the proposed calculation method can achieve great calculation accuracy with a fraction of time of FE simulations, making it suitable to quickly evaluate the performances of a large amount

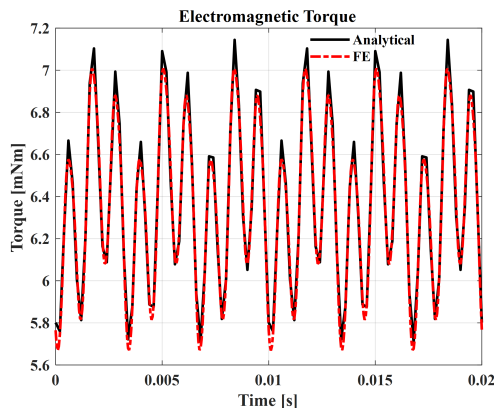


Fig. 5: The calculated instantaneous torque generated by the motor over one electrical cycle, for both analytical and FE calculations.

of motor design candidates, conduct parameter sweeping, and adopt into an optimization routine to identify the optimal motor design.

IV. CONCLUSIONS

In this paper, an improved analytical method for computing the magnetic field and electromagnetic performance of an IPMSM considering the permeability of rotor has been presented. The Laplace and Poisson equations in polar coordinates have been solved using the technique of separation of variables and Fourier series in different subdomains. In order to consider the saturation of the rotor, a general solutions were derived considering the rotor permeability of the pole-piece and the bridge regions, respectively. The analytical solutions can be derived by using the boundary and interface conditions. The electromagnetic performance can be determined analytically based on these solutions. The proposed method was implemented, and the analytical predictions were in good agreement with nonlinear FE simulations.

REFERENCES

- [1] S. Morimoto, "Trend of Permanent Magnet Synchronous Machines," IEEJ Trans. vol. 2, 101–108, 2007
- [2] S. Y. Lim, J. Lee, "A design for improved performance of interior permanent magnet synchronous motor for hybrid electric vehicle", J. Appl. Phys., vol. 99, no. 8, pp. 08R308-1-08R308-3, Apr. 2006.
- [3] J. Kwack, S. Min, J. P. Hong, "Optimal stator design of interior permanent magnet motor to reduce torque ripple using the level set method", IEEE Trans. Magn., vol. 46, no. 6, pp. 2108-2111, Jun. 2010.
- [4] S. Lim, S. Min, J. P. Hong, "Level-set-based optimal stator design of interior permanent-magnet motor for torque ripple reduction using phase-field model", IEEE Trans. Magn., vol. 47, no. 10, pp. 3020-3023, Oct. 2011.
- [5] B. L. J. Gysen, K. J. Meessen, J. J. H. Paulides, and E. A. Lomonova, "General formulation of the electromagnetic field distribution in machines and devices using Fourier analysis," IEEE Trans. Magn., vol. 46, no. 1, pp. 39–52, Jan. 2010.
- [6] L. J. Wu, Z. Q. Zhu, D. A. Staton, M. Popescu, and D. Hawkins, "Comparison of analytical models of cogging torque in surface-mounted pm machines," IEEE Transactions on Industrial Electronics, vol. 59, pp. 2414–2425, June 2012
- [7] B. Hannon, P. Sergeant, L. Dupre, and P. Pfister, "Two-dimensional fourier-based modeling of electric machines — an overview," IEEE Transactions on Magnetics, vol. 55, pp. 1–17, Oct 2019
- [8] Z. Q. Zhu and D. Howe, "Instantaneous magnetic field distribution in brush-less permanent magnet dc motors. iii. effect of stator slotting," IEEE Transactions on Magnetics, vol. 29, pp. 143–151, Jan 1993.
- [9] D. Zarko, D. Ban, and T. A. Lipo, "Analytical calculation of magnetic field distribution in the slotted air gap of a surface permanent-magnet motor using complex relative air-gap permeance," IEEE Transactions on Magnetics, vol. 42, pp. 1828–1837, July 2006.
- [10] Z. Q. Zhu, L. J. Wu, and Z. P. Xia, "An accurate subdomain model for magnetic field computation in slotted surface-mounted permanent-magnet machines," IEEE Transactions on Magnetics, vol. 46, pp. 1100–1115, April 2010.
- [11] K.-H. Shin, H.-I. Park, H.-W. Cho, and J.-Y. Choi, "Analytical prediction for electromagnetic performance of interior permanent magnet machines based on subdomain model," AIP Adv., vol. 7, no. 5, May 2017, Art. no. 056669.
- [12] F. Dubas and K. Boughrara, "New scientific contribution on the 2-d sub-domain technique in polar coordinates: Taking into account of iron parts," Mathematical and Computational Applications, vol. 22, no. 4, 2017
- [13] L. Roubache, K. Boughrara, F. Dubas, and R. Ibtiouen, "Semi-Analytical Modeling of Spoke-Type Permanent-Magnet Machines Considering the Iron Core Relative Permeability: Subdomain Technique and Taylor Polynomial," Progress In Electromagnetics Research B, Vol. 77, 85-101, 2017.